DEVELOPMENT OF FMRI TECHNIQUES FOR PLANNING IN FUNCTIONAL NEUROSURGERY FOR PARKINSON'S DISEASE

M. Mallar Chakravarty, Pedro Rosa-Neto, Scott Broadbent, Alan C. Evans, and D. Louis Collins

McConnell Brain Imaging Centre
Montreal Neurological Institute
3801 University Street, Montreal, Quebec
Canada, H3A 2B4

ABSTRACT

Pre-operative neurosurgical planning often uses data from functional magnetic resonance imaging (fMRI) to identify areas of eloquent cortex, such as the primary and secondary somatosensory cortices, to be spared during surgery. However, the *in-vivo* visualization of subcortical neurosurgical targets has typically involved the warping of subcortical atlases or T2- and diffusion-weighted imaging techniques to help define the anatomical borders. We propose a novel vibrotactile stimulation technique to activate the somatosensory pathway, and particularly the sensory thalamus. Experiments were executed on two MRI scanners (1.5T and 3.0T). A sensitivity analysis demonstrated that statistically significant functional activations of the sensory thalamus can be in achieved in clinically acceptable time (32 minutes at 1.5T and 12 minutes at 3.0T), thus enabling this technique to be used for pre-operative planning in patients.

Index Terms— Image Interpretation - Computer Assisted, Neuronavigation, Magnetic Resonance Imaging, Functional Magnetic Resonance Imaging

1. INTRODUCTION

The pre-operative identification of subcortical targets in functional neurosurgery requires careful planning. In the case of surgical procedures involving the sensory thalamus (such as thalamotomy or deep brain stimulator implantation), *in-vivo* intra-operative functional localization of these structures is used as a surgical gold standard. Typically, different T1- and T2-weighted techniques are constrained by competing factors such as signal-to-noise ratio, resolution, and contrast. Thus image processing and acquisition techniques have been developed to enhance visualization of these nuclei. Anatomical digital atlases derived from serial histological data [4, 26] and print atlases [14, 19, 22] have been used to identify subcortical nuclei. Others have added functional or post-operative data to anatomical representations to help suggest target locations in the sensory thalamus [6, 12] and the subthalamic nucleus [7, 11, 18, 20].

Although subcortical targets are often localized based on distances from visible landmarks [2], anatomical imaging techniques used to visualize subcortical nuclei have grown in popularity. Deoni *et al.* [10] exploit differences in relaxation times of different thalamic nuclei to generate contrast and a constrained field of view to acquire high-resolution images. Tractography techniques from diffusion weighted imaging (DWI) have also been used [1] to derive thalamic segmentations based on cortical connectivity. While other DWI based techniques have been implemented [23], many of these techniques lack the spatial resolution to accurately resolve small structures such as the sensory thalamus.

Here novel vibrotactile stimulation techniques are utilized as a method to elicit somatosensory activations. While most groups report activations of primary and secondary somatosensory cortices, [13, 15–17, 21]; rarely have their been reports of activations of the sensory thalamus [9]. In addition, the time required to achieve significant activations has not been examined. The integration of a digital atlas of the subcortical nuclei to demonstrate the spatial co-localization of the sensory thalamus.

2. MATERIALS AND METHODS

Two different experiments were performed, the first using an 1.5 T MR-scanner, and the second using a 3.0T MR-scanner. The vibrotactile simulator and the two experiments are described in this section. Subjects were immobilized using a vacuum bag and head holder assembly and data was acquired using an eight-channel head coil. During each fMRI experiment, vibrotactile stimulation was delivered 10 seconds into each run to allow for magnetic saturation. A block-design paradigm was employed where stimulation was delivered for 15 seconds and then withheld for 15 seconds until the end of the run. Each four dimensional volume corresponding to an fMRI run was motion corrected using an algorithm which rigidly registers [8] the three-dimensional volume acquired at each repetition time (TR) to the volume acquired at the fourth TR.

Data for each experiment was analyzed for fixed effects in its native space, as only single subject activations are considered in this study. The study was approved by the Research Ethics Committee of the Montreal Neurological Institute and informed consent was obtained from each subject.

2.1. Vibrotactile Stimulation

For the delivery of vibrotactile stimulation a stimulator built at our institute entirely from non-metallic parts was used a described in [5]. The simulator is housed in a large plastic tube, with a delerin rod running through the main axis. Attached to the rod are two fans (at one end) and an offset mass (at the other end). Air flow from an air compressor placed outside of the scanner room is used as the working fluid to cause the fans and offset mass to rotate, thus causing vibration of the entire tube (see Fig. 1). Air-flow at 100psi causes stimulations between 40-50Hz and is regulated using computer operated valves which were controlled using SuperLab Pro (V2.04) software.

Fig. 1. **Vibrotactile simulator used for Experiments A and B.**

2.2. Experiment A: Standard BOLD Acquisition at 1.5 T

Thirteen subjects were used in this experiment (Seven female, age range: 20-60y, mean age: 31.6y, standard deviation of age: 10.2y). All anatomical and functional data was acquired using a Siemens 1.5T Magnetom Sonata system. A T1-weighted anatomical MRI (1 mm isotropic resolution) was acquired using a gradient-echo sequence as an anatomical reference for each subject (TR = 22ms, TE = 9.2ms, and a 30 deg flip angle). Functional data was acquired using a T2*-weighted BOLD sequence (with a 64 x 64 x 64 image voxel matrix at 4mm isotropic resolution, TR = 3.5s, TE = 50 ms, 138 frames, 90 deg flip angle). Four separate runs of functional acquisition were performed, where each run required 8 min and 7 seconds.

The motion corrected functional data (using the method described earlier) was convolved (spatially) using a 6mm full-width-half-maximum Gaussian kernel, before statisitcal analysis (described to Section 2.4).

2.3. Experiment B: High Resolution BOLD Acquisition at 3.0 T

Five subjects were used in this experiment (three female, age range: 25-33y, mean age: 29.2y, standard deviation of age: 3.9y). All anatomical and functional data were acquired using a Siemens 3T Magnetom Trio system. A T1-weighted anatomical MRI (1 mm isotropic resolution) was acquired using a gradient-echo sequence as an anatomical reference for each subject (TR = 23ms, TE = 7.4ms, and a 30 deg flip angle). Functional data was acquired using a T2*-weighted BOLD sequence in coronal slices (with voxel measuring 1.5 mm x 1.5 mm in the acquisition plane and 2.5 mm slice thickness, 128 voxels acquired in each of the 16 coronal slice, TR = 1.3s, TE = 35 ms, 138 frames, 90 deg flip angle). Eight separate runs of functional acquisition were performed, where each run required 3 min. In this case the field of view is limited only to a constrained sub-volume of the brain containing the thalamus,and the primary and secondary somatosensory cortices. The goal was to determine if significant activations could be detected and precisely localized in clinically acceptable time if spatial and temporal resolutions were increased in a constrained region of interest.

The motion corrected functional data (using the method described earlier) was subsequently convolved (spatially) using a 3mm FWHM Gaussian kernel before statistical analysis (described in Section 2.4). A smaller kernel than in Experiment A was used due to the smaller voxel size of the data in this experiment.

2.4. fMRI Data Time Course Analysis

In the experiments described in Sections 2.2 and 2.3 a sensitivity analysis was performed to determine the necessary time required to elicit functional activations of the sensory thalamus. For each run in Experiment A, an analysis of the data from the first run only (A1), from runs one and two (A2), from runs one through three (A3), and all four runs (A4) were performed. Similarly, for Experiment B, a similar analysis was performed yielding analyses B1 through B8. The data was analyzed using the *fmristat* package developed by Worsley *et al* [24]. A statistical summary was estimated for $p<0.05$ [25]. The peak threshold is the lower of the Gaussian Random field theory or Bonferroni corrected threshold and is dependent on the number of voxels in the search area. All voxels above this threshold are considered significant.

2.5. Atlas Integration

To demonstrate how these fMRI techniques can be used with digital atlases the definition of the sensory thalamus defined in the atlas of [4] was extracted and warped to each subject. The atlas-to-subject warping procedure used, is the template based procedure used in [6].

3. RESULTS

Typical results for Experiment A (described in Section 2.2) are shown in Figure 2. Typical results for Experiment B (described in Section 2.2) are shown in Figure 3. For both figures, results are shown for a single subject across runs performed on the right hand. Graphs showing peak t-values in the thalamus, as estimated by *fmristat* are shown in Figure 4. The significance threshold at the voxel level is also shown. Figure shows that at 1.5 T, 6/13 subjects show significant thalamic activation after three runs, 9/13 after 4 runs. At 3.0T, 2/5 show activation after 3 runs and all subjects show significant thalamic activations in runs 4 to 8. Results of the atlas integration for one subject are shown in Figure 5. Amongst those subject demonstrating significant thalamic activation (9/13 in Experiment A and 5/5 in Experiment B), all had peak activations within the atlas definition of the sensory thalamus.

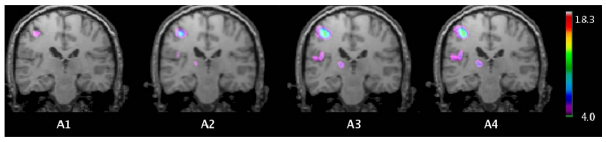

Fig. 2. **Results from Experiment A at 1.5 T described in Section 2.2.** Results from the sensitivity analysis are shown for a single subject are shown.

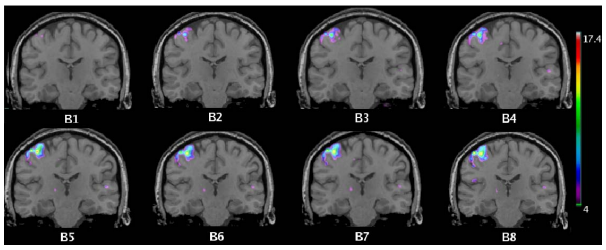

Fig. 3. **Results from Experiment B at 3.0 T described in Section 2.3.** Result from the sensitivity analysis are shown for a single subject.

4. DISCUSSION AND CONCLUSIONS

This paper presents novel techniques for the functional activation of sensory thalamus using fMRI acquisition and analysis techniques. Functional activations of the sensory thalamus were elicited using vibrotactile stimulation and co-localized

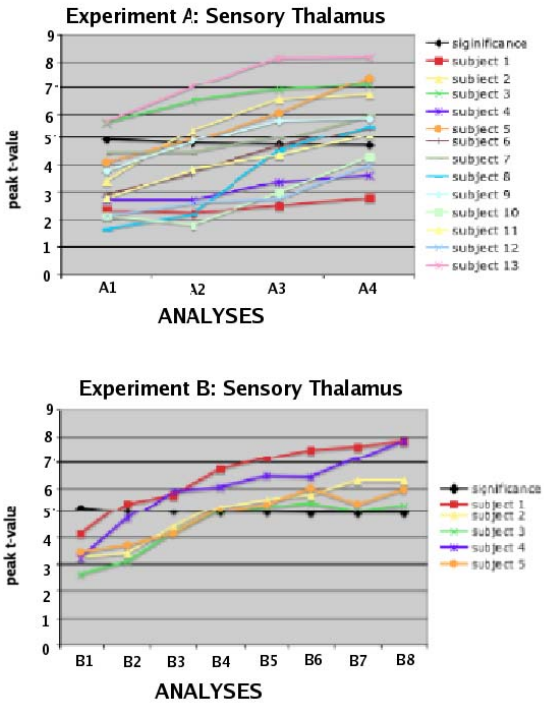

Fig. 4. **Results from Experiments A and B.**. Peak-significance threshold is given for both experiments. Experiment B shows that by increasing both temporal and spatial resolution, significant peak activations of the sensory thalamus can be achieved.

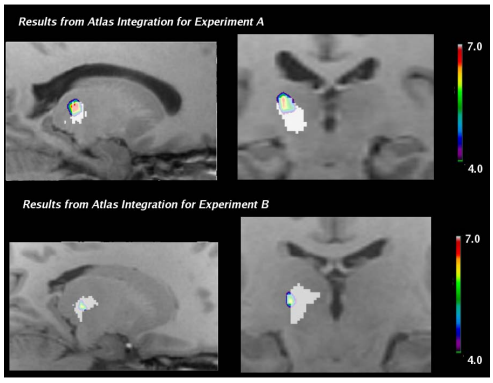

Fig. 5. **Results from atlas integration with functional data from Experiments A and B.**. The opaque white label is the atlas definition of the sensory thalamus, fMRI activations are shown in the spectral colour scheme. Results demonstrate the usefulness of this technique when used in conjunction with an anatomical atlas.

with the definition of the sensory thalamus from a digital atlas of the subcortical nuclei.

The results presented in Section 4 demonstrate significant activations of the sensory thalamus. The results from Experiment A, show that while sensory thalamic activations can be achieved, whole-brain single subject significant activations were not achieved consistently. However, in all subjects tested in Experiment B, single subject activations were achieved within twelve minutes, a length of time suitable for clinical applications. This has important considerations for functional neurosurgical planning where accurate targeting of the sensory thalamus is crucial. By improving the temporal and spatial resolutions, the results demonstrated that single subject functional activations can be achieved.

Figures 2 and 3 show that both techniques yield activations of the primary (S1) and secondary (S2) somatosensory cortices, also of relevance to neurosurgical planning for the removal of tumours encroaching of functionally eloquent areas [3]. Further work will involve a similar time-course analysis as that proposed for the sensory thalamus for S1 and S2.

This technique serves as a method eliciting functional activations, which can serve as complimentary to *in-vivo* imaging techniques presented [10, 2], as well atlas-based planning procedures [6, 4, 26, 19, 12]. Further testing will be required with a patients suffering from movement disorders in order to further evaluate the clinical possibilities for this technique.

5. REFERENCES

[1] T.E.J. Behrens, *et al. Nat, Neurosci.*, 6(7):750–7, 2003.

[2] A.L. Benabid, *et al. Mov. Dis.*, 17(S3):123–9, 2002.

[3] R.G. Bittar *et al. J. Neurosurg.*, 91(6):915–21, 1999.

[4] M.M. Chakravarty *et al. NeuroImage*, 30(2):359–376, 2006.

[5] M.M. Chakravarty *et al.* In *ISMRM*, Berlin, Germany, 2007.

[6] M.M. Chakravarty *et al.* In *MICCAI 2005*, volume 2 of *Lecture Notes in Computer Science*, pages 394–401, Springer.

[7] M.M. Chakravarty *et al.* In *MICCAI 2006*, volume 2 of *Lecture Notes in Computer Science*, pages 389–396, Springer.

[8] D.L. Collins *et al. JCAT*, 18(2):192–205, March 1994.

[9] K.D. Davis *et al. J. Neurophys.*, 80(3):1533–1546.

[10] S.C.L. Deoni *et al. Mag. Res. Med.*, 53(1):237–41, 2005.

[11] P.F. D'Haese *et al. IEEE TMl*, 24(11):1469–1478, 2005.

[12] K.W. Finnis *et al. IEEE TMI*, 22(1):93–104, January 2003.

[13] S.T. Francis *et al. NeuroImage*, 11(3):188–202, 2000.

[14] K.A. Ganser *et al. MedIA*, 8(1):3–22, 2004.

[15] P.A. Gelnar *et al. NeuroImage*, 7(4 Pt 1), 1998.

[16] S.M. Golaszewski *et al. NeuroImage*, 17(1):421–30, 2002.

[17] S.J. Graham *et al. Mag. Res. Med.*, 46(3):436–42, 2001.

[18] T. Guo *et al.* In *MICCAI 2005*, volume 1 of *Lecture Notes in Computer Science*, pages 835–842, Springer.

[19] W.L. Nowinski *et al. IEEE TMI*, 19(1):62–69, January 2000.

[20] F.J. Sanchez Castro *et al. Int. J. of CARS*, 25(1):1440–1450, 2006.

[21] R.J. Seitz and P.E. Roland. *Acta Neurol. Scand.*, 86(1):60–67, 1992.

[22] P. St-Jean *et al. IEEE TMI*, 17(5):854–866, May 1998.

[23] M.R. Wiegell *et al. NeuroImage*, 19:391–401, 2003.

[24] K.J. Worsley *et al. Neuroimage*, 15:1–15, 2002.

[25] K.J. Worsley *et al. HBM*, 4:58–73, 1996.

[26] J. Yelnik *et al. NeuroImage*, 34:618–638, 2007.